

PAPER • OPEN ACCESS

Digital holographic study of vapor transport of heavy hydrocarbon from heated well cavity

To cite this article: Digvijay Shukla and Pradipta Kumar Panigrahi 2021 *J. Phys.: Conf. Ser.* **2116** 012079

View the [article online](#) for updates and enhancements.

You may also like

- [How to Identify Exoplanet Surfaces Using Atmospheric Trace Species in Hydrogen-dominated Atmospheres](#)
Xinting Yu, , Julianne I. Moses et al.
- [Research and application of efficient milling process for surface casing](#)
Xu Zhang, Jianning Wang, Changqing Ma et al.
- [Multi-Vt Performance Dependence on Capping Layer Position by NPT for PMOS Device Applications](#)
Jiaxin Yao, Zhenhua Wu and Huaxiang Yin



The Electrochemical Society
Advancing solid state & electrochemical science & technology

242nd ECS Meeting

Oct 9 – 13, 2022 • Atlanta, GA, US

Early hotel & registration pricing
ends September 12

Presenting more than 2,400
technical abstracts in 50 symposia

The meeting for industry & researchers in

BATTERIES
ENERGY TECHNOLOGY
SENSORS AND MORE!



**ECS Plenary Lecture featuring
M. Stanley Whittingham,**
Binghamton University
Nobel Laureate –
2019 Nobel Prize in Chemistry



Digital holographic study of vapor transport of heavy hydrocarbon from heated well cavity

Digvijay Shukla and Pradipta Kumar Panigrahi*

Department of Mechanical Engineering, Indian Institute of Technology Kanpur,
Kanpur 208016, India.

*Corresponding author: panig@iitk.ac.in

Abstract. Thin film evaporative cooling is one of the liquid cooling technologies, capable of removing high heat flux with lower junction temperature due to the utilization of latent heat of vaporization. To understand the various transport processes involved in vapour phase during thin film evaporation, evaporation from a heated well cavity of diameter 3 mm and height 2 mm is studied using Digital holographic interferometry technique. A flat disk-shaped vapour cloud is appeared for heated as well as not- heated well surface case. This signifies radial outward natural convection instead of pure diffusion. A higher vapour concentration is obtained at each time instants for heated surface case due to the higher evaporation rate as compared to non-heated, ambient case.

1. Introduction

Electronic cooling has become a serious design concern while designing the next generation high performance electronic i.e., microprocessors, Radars, Laser diodes etc. As the number of transistors are increasing heat generation inside the chip also increases and the heat flux from the device is reaching a magnitude of an order of 1000 W/cm^2 . Conventional air-cooling technologies are not capable of removing such a high heat flux.

Much larger heat flux can be dissipated while keeping the junction temperature below an allowable limit by utilizing the phase change heat transfer via evaporation from a free liquid surface of thin film over a heated chip [1-3]. So, the thin film heat transfer has been studied by the many researchers to get understanding of this complex phenomenon. Thin film evaporation is different from the boiling as phase change occurs at the free surface of liquid instead of nucleation at the heater surface as in case of boiling. Now the rate of evaporation from a thin liquid film depends upon conduction and convective heat transfer within the film and mass transfer in vapor phase from the liquid-vapor interface. Various convective flow i.e., buoyancy induced convection and Marangoni convection also influences the convective heat transfer resistance. So, the understanding of vapor phase transport from a thin liquid film evaporating from a heated surface is necessary to reveal the underlying physics of the process.

2. Problem Statement

In present work digital holographic interferometry technique is used to study the effect of well bottom surface (substrate) temperature on the evaporation and vapor phase transport of a heavy volatile hydrocarbon from circular well cavity of small depth. Vapour cloud of liquid evaporating from the heated well cavity is compared with the non-heated case. Spatial as well as temporal characteristics of



vapor cloud originating from a circular well cavity whose bottom surface is heated ($35\text{ }^{\circ}\text{C}$) is compared with non- heated case where well bottom surface is kept at ambient temperature.

3. Methodology

The layout of the experimental setup is shown in figure 1(a). A Mach-Zehnder interferometer with finite fringe setting has been used. The laser beam is divided into two beams by the first beam splitter which splits the beam into an object and a reference beam as shown in figure 1(a). The object beam is passed through the vapor cloud originating from the well cavity while reference beam passes through the ambient air. Finally, these two beams are recombined by the second beam splitter and hologram is recorded on a CCD camera (782×582 pixels with resolution of $8.30\text{ }\mu\text{m}$) using a Zoom lens. The Schematic of heated well cavity setup has been shown in figure 1(b).

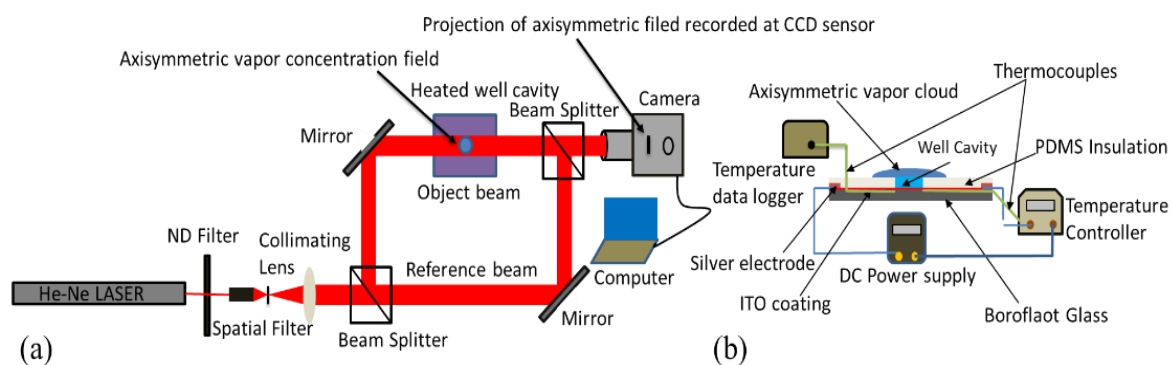


Figure 1. (a) Mach-Zehnder interferometer setup and (b) Heated well cavity setup.

A 5 mm external and 3 mm internal diameter plexiglass capillary of height 2 mm is fixed by an epoxy glue on an ITO coated side of Borofloat glass ($25\times 25\times 1.1\text{ mm}^3$) substrate. Bottom surface of the well cavity is resistively heated by passing current through a DC power supply. Two T type thermocouples are placed at the bottom of well surface. One thermocouple is connected to the temperature controller (SELEC 320) as a feedback signal to precisely control the bottom surface of the well while other one is used to record the temperature change during evaporation. PDMS insulating layer is casted around the capillary to reduce the heat loss from the substrate. Constant well bottom surface temperature of $35\text{ }^{\circ}\text{C}$ is maintained for heated surface case. Ambient pressure and temperature were 1 atm and $18\pm 0.5\text{ }^{\circ}\text{C}$, respectively.

Before filling the liquid inside heated well cavity, interferometer is set to the wedge fringe setting and reference hologram is recorded. After this cyclohexane is filled inside the cavity by a micropipette and holograms are recorded at the time interval of 1 sec until liquid is fully evaporated from the cavity. A Fourier Transform Profilometry [4] algorithm is used to extract the phase at each pixel of the image. The phase of each pixel of object hologram is then extracted and subtracted from the phase of reference hologram of same pixel. This yields the total phase shift at each pixel for an object hologram. But the obtained phase shift is called wrapped phase difference as the phase shift values lies only between 0 to 2π . This wrapped phase is then unwrapped by Goldstein algorithm [5]. This unwrapped phase shift ($\Delta\phi$) is proportional to the optical path difference created when the laser beam passes through the refractive index field above the well cavity.

The obtained unwrapped phase field needs to be tomographically reconstructed to obtain the three-dimensional refractive index field. Since field above the well cavity is axis-symmetric, an inverse Abel inversion can be applied to unwrapped phase, to yield a 2D cut of refractive index field [6]. The refractive index difference field (Δn) at a given height z is given by:

$$\Delta n(r) = \frac{-\lambda}{2\pi^2} \int_r^\infty \frac{\Delta\phi'(x)}{\sqrt{(x^2 - r^2)}} dx \quad (1)$$

Here, λ is wavelength of laser beam and $\Delta\phi'(x)$ is first order derivative of unwrapped phase shift. Fourier- Hankel algorithm is used for Abel inversion [7]. Finally, this refractive index field is converted into vapour mole fraction field (χ). Following equation can be used for relating refractive index difference field with unknown local temperature (T) and mole fraction [6].

$$\chi = \frac{1}{\Delta n_{ref}} \frac{T}{T_{amb}} \left[\Delta n - (n_a - 1) \left(\frac{T_{amb}}{T} - 1 \right) \right] \quad (2)$$

$\Delta n_{ref} = (n_v - n_a)$, here n_v (1.001728) and n_a (1.0002743) are the refractive index of pure vapor of liquid and air respectively at ambient temperature (T_{amb}) and pressure [8]. If temperature impact is marginal, then equation (2) reduces to $\chi = \Delta n / \Delta n_{ref}$. Detailed procedure of digital holographic data analysis can be found in ref [9].

4. Results and discussion

In figure 2 wrapped phase maps of cyclohexane evaporating from circular well cavity are compared for non-heated and heated case at the start of evaporation ($t \sim 0$ sec). Due to the heated bottom surface evaporation of liquid is higher and more vapour of cyclohexane is present in the vapour phase, which resulted in higher change in refractive index and eventually more iso-concentration contours are present in the heated bottom surface case (figure 2b) as compared to non-heated case, where bottom surface is maintained at ambient temperature.

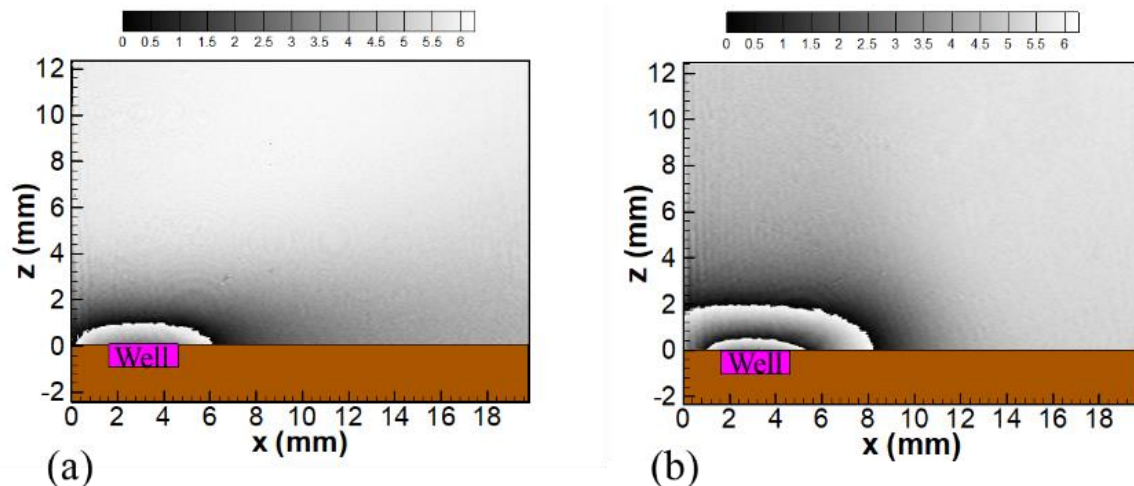


Figure 2. Wrapped phase map at initial time ($t \sim 0$ sec) of evaporation (a) at ambient temperature and (b) at 35 °C.

Figure 4 compares vapour mole fraction fields at various non-dimensional time instants ($t^* = t/t_e$, where t_e is total time of evaporation) for non-heated and heated case. Since liquid is heavier than the surrounding medium a flat disk shaped vapour cloud is obtained instead of hemispherical vapour cloud, which forms in case of pure diffusion limited case as can be seen in figure 4.

At every time instants vapour concentration is higher for the heated bottom surface case and spread of cloud in radial direction is also higher in heated case. This can be clearly seen in figure 3a where vapor mole fraction is plotted along a line in radial direction at the top surface of well ($z = 0$) at various time instant for both cases. Figure 3b shows the variation of refractive index change in normal direction at the center of the well ($r = 0$) at various time instants. It shows that vapour concentration is always higher for the for heated case in both radial and normal directions irrespective of time. Higher

values of vapor mole fraction in case of heated cavity can increase the density gradient required for the natural convection in the vapor phase which can lead to the higher evaporation rate compared to pure diffusion model even for the smaller radius droplets/cavity.

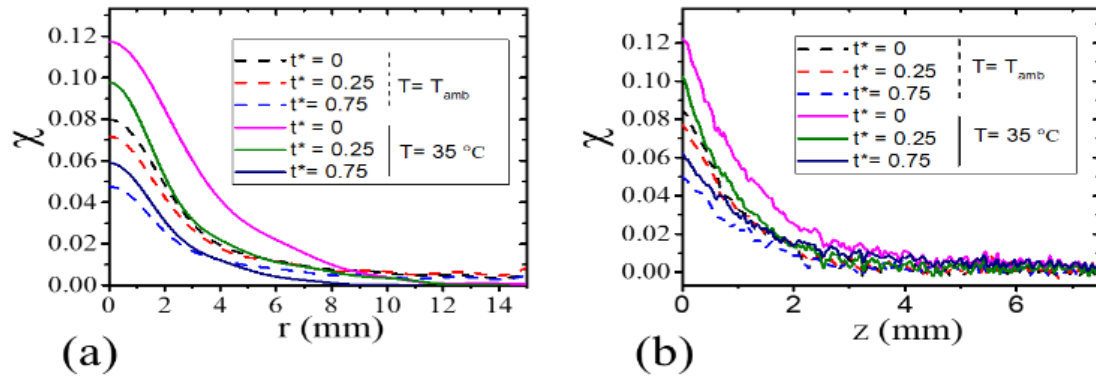


Figure 3. The refractive index (Δn) profile for different normalized time instants ($t^* = t/t_e$): (a) at the surface of the well ($z = 0$), along the radial direction and (b) at center of the well ($r = 0$), along the normal direction.

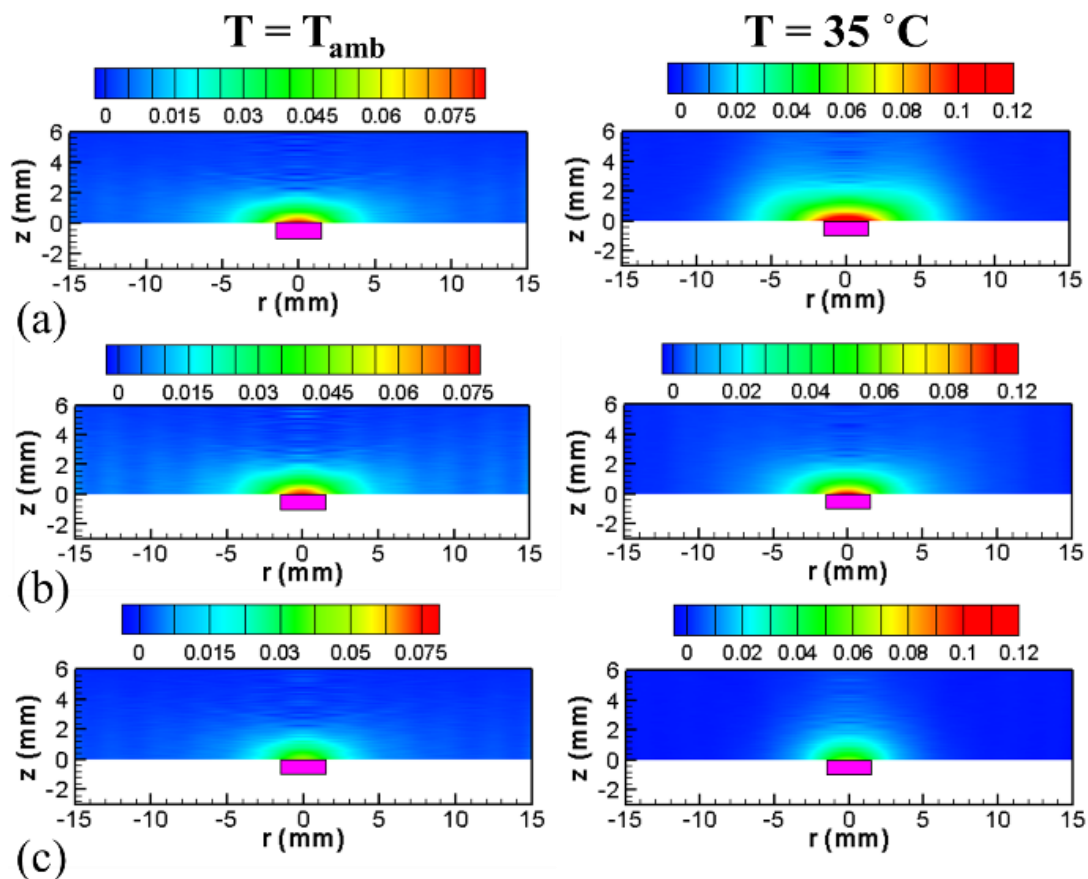


Figure 4. Vapor mole fraction maps at various time instants. Left- hand side represents the case when well bottom surface is maintained at ambient temperature while for right- hand side, well bottom surface temperature is kept at 35°C (a) $t^* = 0$, (b) $t^* = 0.25$ and (c) $t^* = 0.75$.

5. Conclusion

A flat disk-shaped vapour cloud is obtained for heated as well as non-heated well surface case. This signifies the presence of radial outward convection instead of pure diffusion. A higher vapour mole fraction is obtained at each time instants for heated surface case because of higher evaporation rate as compared to non-heated, ambient case. This may lead to the higher convective contribution on evaporation rate.

Acknowledgments

Authors acknowledge the support from Ministry of Electronics and Information Technology, Government of India.

References

- [1] Ohadi M, Qi J and Lawler J 2005 *Microscale Heat Transfer Fundamentals and Applications: Springer* 321-338.
- [2] Kabov OA, Zaitsev D, Cheverda V and A Bar-Cohen 2011 *Experimental Thermal and Fluid Science* **35** 825-831.
- [3] Narayanan S, Fedorov AG and Joshi YK 2009 *Nanoscale and Microscale Thermophysical Engineering* **13** 30-53.
- [4] Takeda M, Ina H and Kobayashi S 1982 *JosA* **72** 156-160.
- [5] Goldstein RM, Zebker HA and CL Werner 1988 *Radio science* **23** 713-720.
- [6] Dehaeck S, Rednikov A and Colinet P 2014 *Langmuir* **30** 2002-2008.
- [7] Ma S, Gao H and Wu L 2008 *Applied optics* **47** 1350-1357.
- [8] Gardiner W Jr, Hidaka Y and Tanzawa T 1981 *Combustion and Flame* **40** 213-219.
- [9] Shukla D and Panigrahi PK 2020 *Applied optics* **59** 5851-5863.